DOI: https://doi.org/10.46632/mc/1/2/13

Materials and its Characterization
Vol: 1(2), 2022
REST Publisher; ISBN: 978-81-948459-0-4
Website: http://restpublisher.com/book-series/materials-and-its-characterization/

Investigation of Laser Material Potential in Lead Tungsten Tellurite Glasses

A Mohan Babu
Audisankara College of Engineering & Technology Nellore, Andhra Pradesh, India
*Corresponding author Email: mohanphy57@gmail.com

***Abstract**: Lead tungsten tellurite (LTT) glasses, incorporating varying concentrations of Dy3+ions, were synthesized and subjected to comprehensive characterization encompassing optical absorption, photoluminescence, and decay measurements. X-ray diffraction (XRD) analysis affirmed the amorphous nature of the LTT host. Employing the Judd–Ofelt (J–O) theory, three phenomenological intensity parameters $\Omega_\lambda(\lambda = 2, 4, 6)$ were derived from absorption spectral intensities. The heightened sensitivity of the $^6H_{15/2}\rightarrow{}^6F_{11/2}$ transition, determined by the magnitude of the Ω_2 parameter, was explored. Radiative properties, including spontaneous transition probabilities (A_R), fluorescence branching ratios (β_R), and radiative lifetimes (τ_R), were determined using the J–O intensity parameters. The impact of Dy3+ion concentration on the emission intensities of $^4F_{9/2}\rightarrow{}^6H_J$ (J = 15/2, 13/2, 11/2, and 9/2) transitions was also investigated and reported.*

***Keywords:** optical absorption, X-ray diffraction, photoluminescence.*

1. Introduction

In exploring the influence of the host material on the lasing capabilities of rare-earth ions, various glass matrices, such as fluorides, phosphates, borates, fluorophosphates, fluoroborates, fluorozirconates, sulphides, selenides, and tellurites, have undergone thorough investigation [1–11]. Recent research has focused on tellurite and heavy metal oxide glasses doped with rare-earth ions due to their high refractive indices, low phonon energies, and strong solubility in rare-earth ions, highlighting their photoluminescence characteristics [12]. Host glasses with low-phonon energy often exhibit enhanced fluorescence quantum efficiencies and reduced non-radiative relaxation rates. Tungsten-based materials are well-recognized for their electrochromic and photochromic properties, finding diverse applications in smart windows, display panels, and sensors [13–15]. Additionally, the incorporation of lead fluoride (PbF_2) serves to lower the host characteristics. In the characterization of laser glasses, understanding the transition probabilities of 4f–4f transitions involving rare-earth ions is crucial. Dy3+ions, incorporated into diverse glasses and crystals, have been a focus among trivalent lanthanides for generating dual-color (blue or yellow) luminescent materials. This stems from their blue emission in the range of 470–500 nm, corresponding to the $4F_{9/2}\rightarrow{}^6H_{15/2}$ transition, and their yellow emission in the range of 570–600 nm, corresponding to the hypersensitive transition $^4F_{9/2}\rightarrow{}^6H_{13/2}$. Consequently, the yellow-to-blue (Y/B) luminescence intensity ratio can be modified by altering the host glass, Dy^{3+}content, chemical composition, excitation wavelengths, and heat treatment—all of which contribute to the production of white light [9].The investigation employed a host composition based on tellurite, specifically TeO_2-WO_3-PbF_2, to examine the unique visual emission patterns of Dy^{3+}ions arising from the $^4F_{9/2}\rightarrow{}^6H_J$ (J = 15/2, 13/2, 11/2, and 9/2) transitions. This study details the spectroscopic analyses of Lead Tungsten Tellurite (LTT) glasses, incorporating varying concentrations of Dy^{3+}ions, and explores their luminescence properties concerning the generation of vibrant yellow (586 nm) and blue (484 nm) emissions.

2. Experimentation Methods

Synthesis of glasses with the molar composition (in mol %) of $^{15}PbF_2$ + $^{25}WO_3$ + (60−x)TeO_2 + xDy_2O_3 (where x = 0.1, 0.5, 1.0, and 2.0) was achieved through the melt quenching technique. The resulting glasses were designated as LTTDy01, LTTDy05, LTTDy10, and LTTDy20 glasses, respectively. TeO_2, WO_3, PbF_2, and Dy_2O_3 starting materials were meticulously blended in an agate mortar to create a homogeneous mixture, which was then subjected to melting in an electric furnace for 40 minutes at 700–750 °C in a platinum crucible. Following the casting of the melt into a pre-prepared brass mold, annealing was carried out at 300 °C for 12 hours to alleviate thermal stresses, followed by gradual cooling to ambient temperature.
A Siefert X-ray diffractometer, employing CuKα radiation at 40 kV and 30 mA, confirmed the amorphous nature of the samples. Density measurements, following Archimedean's principle, were conducted with xylene as the immersion solvent. Refractive index measurements utilized a 2 mW He-Ne polarized laser (632.9 nm) and the Brewster's angle technique. For LTTDy10 glass, the observed refractive index and density were 2.2326 and 6.569 g/cm³, respectively. Absorption spectra in the 700–2100 nm range were obtained using a Varian Cary 5E UV-vis-NIR spectrophotometer. Excitation (em = 576 nm), photoluminescence (ex = 452 nm), and decay (λ_{em} = 576 nm and λ_{ex} = 452 nm) measurements were performed with a JOBIN YVON Fluorolog-3 spectrofluorimeter equipped with xenonflash lamp as light source.

Concepts

The absorption spectra of lanthanides are attributed to intraconfigurational f-f transitions, primarily of the induced electric dipole type. The representation of absorption band intensities can be achieved through the area approach and the formula [16], expressing them in relation to the measured oscillator strengths (f_{meas}).

$f_{meas} = 4.32 \times 10^{-9}\int\varepsilon(v)dv$ (1)

Therefore, the application of Beer-Lambert's law allows for the derivation of ε(v), representing the molar absorptivity at energy v (cm^{-1}). The Judd-Ofelt (J-O) model [17, 18] is employed for the theoretical calculation of the intensities associated with intraconfigurational f-f transitions of lanthanide ions. According to this model, the transition intensities are characterized by three phenomenological parameters Ω_λ (λ = 2, 4, 6), known as J-O intensity parameters, which are contingent on the local environment. These parameters define the computed oscillator strengths (f_{cal}) for transitions from the starting state J to the final stateψ J .

Therefore, the application of Beer-Lambert's law allows for the derivation of ε(~), representing the molar absorptivity at energy ~ (cm−1). The Judd-Ofelt (J-O) model [17, 18] is employed for the theoretical calculation of the intensities associated with intraconfigurational f-f transitions of lanthanide ions. According to this model, the transition intensities are characterized by three phenomenological parameters Ω_λ (λ = 2, 4, 6), known as J-O intensity parameters, which are contingent on the local environment. These parameters define the computed oscillator strengths (f_{cal}) for transitions from the starting state J to the final state {ψ´J´}.Formulas can be employed to calculate the radiative lifetime (τ_R) of an excited state, luminescence branching ratios (β_R) for diverse emissions originating from the same initial level, and stimulated emission cross-sections (σ_e) following

where Δλp denotes the emission band's effective bandwidth and λp indicates its peak wavelength.

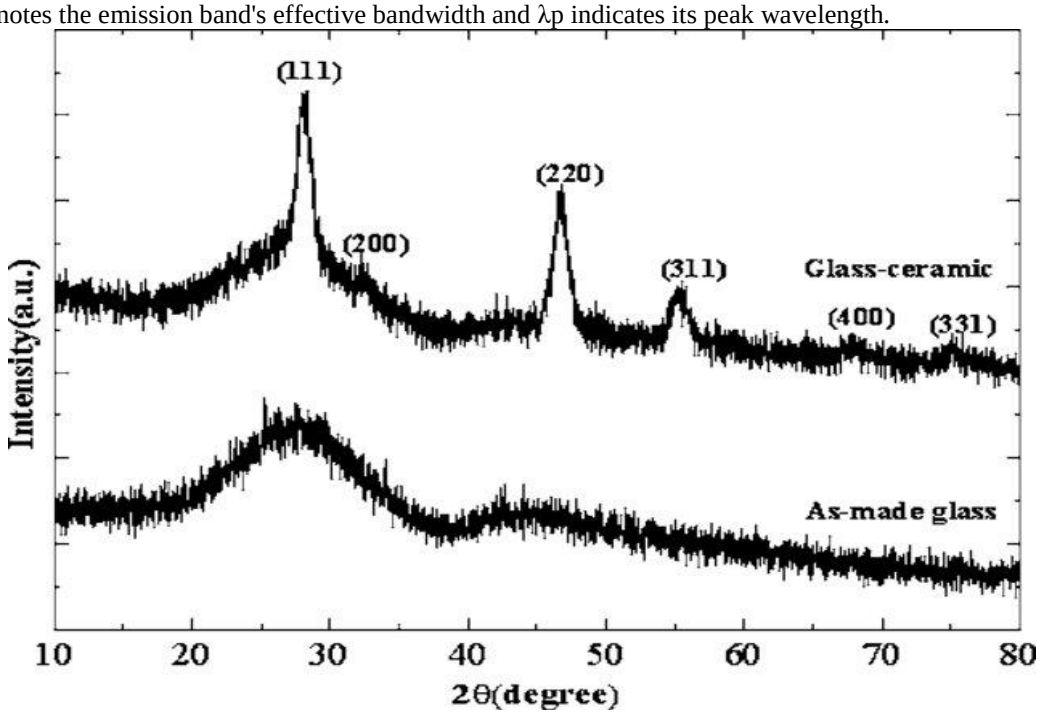

FIGURE 1. XRD profiles LTTDy10 [3]

3. Results and discussion

Glassy nature

Examinations utilizing X-ray diffraction have been carried out to distinguish between the crystalline and non-crystalline structures of LTTDy glasses. The XRD readings for all samples exhibit comparable patterns, and Fig. 1 illustrates the XRD profile of LTTDy10 glass for comparison. While there are no noticeable intensity peaks in the XRD patterns, the broad scattering at low angles suggests the glassy/amorphous nature of the LTT glass system.

Spectroscopic characteristics and J-O evaluation

The absorption spectra of LTTDy10 glass, recorded at room temperature within the wavelength range of 700–2100 nm, are presented in Fig. 2. Each absorption peak signifies the transition of the Dy^{3+}ion's excited states from its ground state, $^6H_{15/2}$. The spectra comprise six distinct and non-uniform wide absorption bands at 753, 802, 905, 1092, 1275, and 1685 nm. These bands correspond to the $^6H_{15/2}\rightarrow{}^6F3/2$, $^6F_{5/2}$, $^6F_{7/2}$, $^6F_{9/2}$, $^6F_{11/2}$, and $^6H_{11/2}$ transitions, respectively. The absorption transition assignments, as detailed in Table 1, align with the work of Carnall et al. [19].

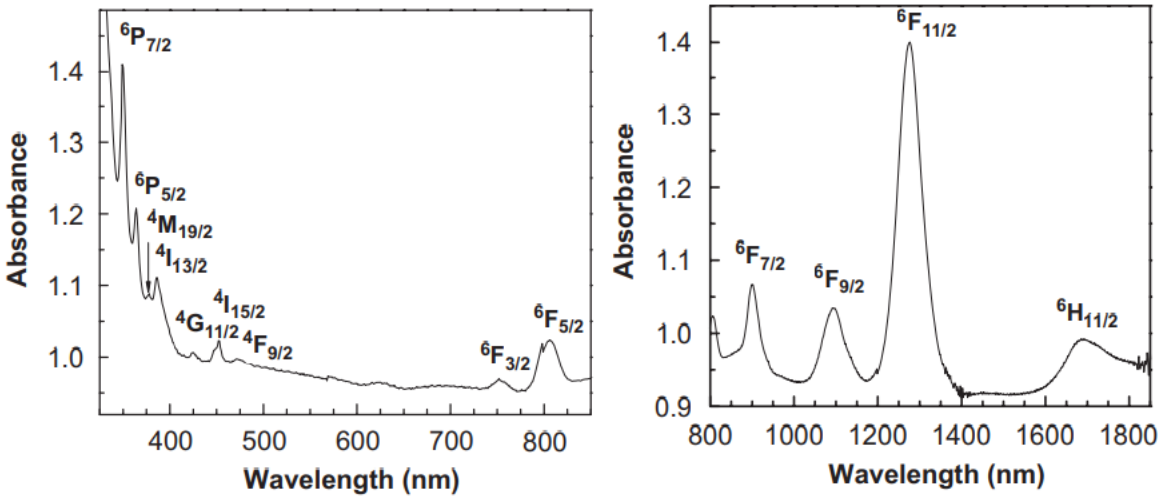

FIGURE 2. Absorbance and wavelength [4]

The measured oscillator strengths (f_{meas}) for various observed absorption bands were determined using Eq. (1). Judd–Ofelt analysis was conducted on the measured oscillator strengths, employing., to derive the calculated oscillator strengths (f_{cal}) and consequently the J–O intensity parameters. A notably small root mean square (δ_{rms}) deviation of ±0.34×10−6 signifies a robust agreement between the measured and calculated oscillator strengths (refer to Table 1), affirming the precision of J–O intensity parameters (Ω_λ). Table 2 provides a comparison of J–O intensity parameters across different glass matrices. The magnitudes of Ω_λ values indicate that the trends in intensity parameters primarily rely on the ligand environment surrounding the rare-earth ion. As suggested by Jorgensen and Reisfeld [20], the Ω_2 parameter's magnitude is contingent on the covalence of the metal–ligand bond and the asymmetry of ion sites near the rare-earth ion, while the magnitudes of Ω_4 and Ω_6 parameters are linked to the rigidity of the medium in which the ions are situated. The assessed Ω_2 parameter for LTTDy10 glass aligns well with values obtained for tellurite [21,22] and lead borate [7,23] glasses. Due to the inhomogeneity of the host around the rare-earth ions, certain absorption band intensities of each rare-earth ion are notably sensitive to the ligand environment. These transitions adhere to the selection rules $\Delta S=0, |\Delta L| \leq 2$, $|\Delta J| \leq 2$ and are identified as hypersensitive transitions [24]. Hypersensitive transitions are characterized by large values of the reduced matrix elements $\|U^2\|$, and the degree of hypersensitivity is predominantly described by the magnitude of the intensity parameter [17]. The relative variation of the Ω_2 parameter for a rare-earth ion in different environments serves as a measure of the degree of hypersensitivity exhibited by that ion. For the Dy^{3+}ion, the $^6H_{15/2}\rightarrow{}^6F_{11/2}$ transition is the hypersensitive transition. Generally, the intensity of the hypersensitive transition is higher when compared to other transitions in any host medium. The $^6H_{15/2\rightarrow}{}^6F_{11/2}$ hypersensitive transition in LTTDy10 glass exhibits a higher magnitude of f_{meas}value.

Spectra of excitation and photoluminescence

To analyze the luminescence properties concerning the activator (Dy^{3+}) concentration, it is essential to determine the appropriate excitation wavelength for the ion. To achieve this, the excitation spectrum recorded for LTTDy10 glass, with emission monitoring at 576 nm, is depicted in Fig. 3. A total of six excitation bands are identified at 352, 365, 388, 426, 452, and 472 nm, corresponding to the $^6H_{15/2}\rightarrow{}^5P_{7/2}$, $^5P_{9/2}$, $^4F_{7/2}$, $^4G_{11/2}$, $^4I_{15/2}$, and $^4F_{9/2}$ transitions, respectively. The two excitation bands related to the $^6H_{15/2}\rightarrow{}^4I_{15/2}$ and $^6H_{15/2}\rightarrow{}^4F_{9/2}$ transitions are not distinctly resolved due to the small energy gap of ~938 cm−1 between the $^4I_{15/2}$ and 4F9/2 levels. Given that the excitation band corresponding to the $^6H_{15/2}\rightarrow{}^4I_{15/2}$ (452 nm) transition is more prominent, all LTT glasses were excited with 452 nm to record the photoluminescence spectra. Figure 4 displays the photoluminescence spectra of LTTDy01, LTTDy05, LTTDy10, and LTTDy20 glasses. The spectra feature two relatively intense emission bands: 4F9/2→$^6H_{15/2}$(484 nm) and 4F9/2→6H13/2 (576 nm), along with two considerably weaker bands: 4F9/2→6H11/2 (665 nm) and 4F9/2→6H9/2 (750 nm) transitions.

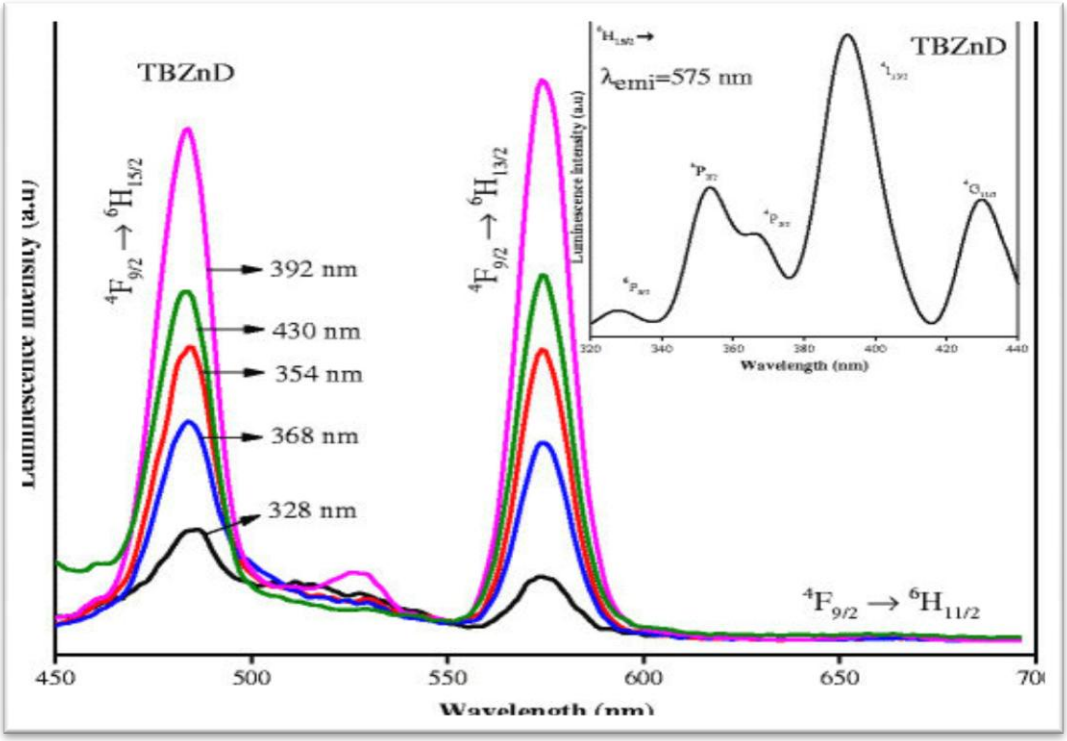

FIGURE 3. NIR spectra of LPDy glass title [5]

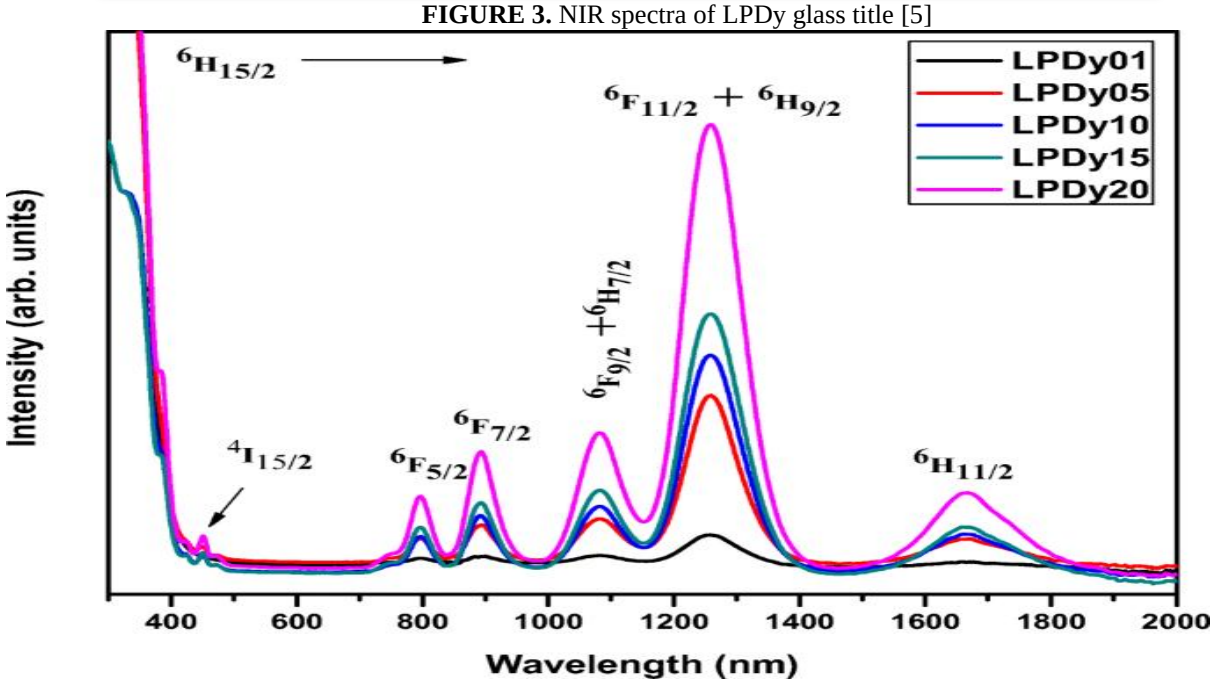

FIGURE 4. Photoluminescence spectra of LTT glasses at various Dy3+ion concentrations [6]

The 4F9/2→6H13/2 transition identified in the yellow region is a hypersensitive transition following the selection rules J = ±2 and L = ±2 [24]. Consequently, the intensity of this transition is strongly influenced by the surrounding environment. The inset of Fig. 4 illustrates the emission channels of Dy^{3+}ions in the LTT glass system. The 452 nm excitation wavelength elevates Dy3+ions to the 4I15/2 level. Due to the small energy gap between the 4I15/2 and 4F9/2 states, the excited Dy^{3+}ions rapidly populate the 4F9/2 meta-stable state through a fast non-radiative decay process. Radiative transitions from the 4F9/2 excited state to its lower-lying 6HJ (J = 15/2, 13/2, 11/2, and 9/2) states occur, emitting radiation at 484, 576, 665, and 750 nm. With a 452 nm excitation, the emission of radiation from the LTTDy glasses appears as yellowish-white, primarily due to the large yellow-to-blue (Y/B) intensity ratio. In this investigation, the Y/B ratios are found to be 0.92, 1.00, 1.02, and 1.21 for LTTDy01, LTTDy05, LTTDy10, and LTTDy20 glasses.

Quenching of luminosity and covalence of Dy–O bonds

To achieve intense luminescence from an activator ion in any host medium, its concentration must be optimized. To optimize the Dy^{3+}ion concentration in the LTT glass host, the photoluminescence spectra recorded for LTTDy01, LTTDy05, LTTDy10, and LTTDy20 glasses are presented in Fig. 4. Luminescence intensity increases with the rise in Dy^{3+}ion concentration from 0.1 to 1.0 mol%; however, a decrease in luminescence intensity is observed for 2.0 mol%, attributed to the increasing interaction among Dy^{3+}ions at higher concentrations. The variation of luminescence intensity for the $^4F_{9/2} \rightarrow {}^6H_{13/2}$ transition

with Dy^{3+}ion concentration is also depicted (solid line). This graph indicates that the luminescence intensity ofDy^{3+}ions in the LTT glass host is highest at a concentration of 1.25 mol%. This result suggests that LTT glasses doped with 1.25 mol% of Dy^{3+}ions can exhibit intense luminescence upon 452 nm excitation.To assess the degree of covalence in the Dy–O bond, the variation of the yellow-to-blue (Y/B) intensity ratio for the $^4F_{9/2}\rightarrow{}^6H_{13/2}$ and $^4F_{9/2}\rightarrow{}^6H_{15/2}$ transitions at different Dy^{3+}ion concentrations is plotted against Dy^{3+}ion concentration. Higher Y/B intensity ratios indicate a greater degree of covalence between dysprosium and oxygen ions [23]. The evaluated Y/B intensity ratios reveal that Dy–O covalence increases with the rise in Dy^{3+}ion concentration in LTT glasses.

Emission of white light

The creation of white light, along with the generation and control of different colors in solid-state display devices, often involves appropriate combinations of blue (B) and yellow (Y) emissions [25–27]. The potential for white light generation in LTTDy glasses has been analyzed using chromaticity color coordinates. In the present study, the calculated color coordinates are (0.39, 0.44); (0.37, 0.43); (0.34, 0.40); and (0.38, 0.43) for LTTDy01, LTTDy05, LTTDy10, and LTTDy20 glasses, respectively. All these coordinates fall within the white light region of the CIE 1931 chromaticity. Across all concentrations, the deviation in the coordinates is minimal, indicating consistent white light generation.

Radiative characteristics

The J–O intensity parameters (Ω_λ) derived for LTTDy10 glass have been utilized to estimate various radiative parameters through Eqs. (3)–(6). This approach aims to predict the efficient luminescence characteristics of two intense transitions, namely $^4F_{9/2}\rightarrow{}^6H_{13/2}$ and $^4F_{9/2}\rightarrow{}^6H_{15/2.}$ The calculated radiative transition probabilities (A_R), fluorescence branching ratios (β_R), stimulated emission cross-sections (σ_e), and optical gain parameters ($\sigma_e\times\tau_R$), as presented align well with values reported in the literature [7,21,23,28,29]. Branching ratios and stimulated emission cross-sections are crucial laser parameters that indicate the luminescence efficiency of the host material. In this study, it is observed that the values of branching ratio (τ_R) and stimulated emission cross-section (σ_e) for the $^4F_{9/2}\rightarrow{}^6H_{13/2}$ transition are maximum among all other transitions. The higher magnitudes of branching ratio and stimulated emission cross-section for the $^4F_{9/2}\rightarrow{}^6H_{13/2}$ transition suggest its suitability for achieving laser action in LTTDy10 glass. Additionally, the optical gain parameter ($\sigma_e\times\tau_R$), which serves as a measure of the laser threshold, is also larger than that of barium fluoroborate glass [29].

Analysis of fluorescence decay

The decay curves of the $^4F_{9/2}$ excited state were examined for various Dy^{3+}ion concentrations, revealing a single-exponential nature for all concentrations. The measured lifetimes (τ^{meas}), determined by the first e-folding times of the decay curves, are 248, 226, 152, and 146 s for LTTDy01, LTTDy05, LTTDy10, and LTTDy20 glasses, respectively. The decrease in τ_{meas} values with the increase in Dy^{3+}concentration is primarily attributed to the growing interaction among Dy3+ions at higher concentrations. The insetillustrates the variation of τ_{meas} values with Dy3+concentration. The measured lifetime (152 s) of the $^4F_{9/2}$ level in LTTDy10 glass is found to be higher than those reported for borate (140 s) [30], phosphate (100 s) [30], and fluorozirconate (120 s) [31] glasses. The predicted radiative lifetime (τ_R) of the $^4F_{9/2}$ excited level, obtained from J–O theory [17,18], is 377 s. The considerable difference between the magnitudes of $\tau_R$andτ_{meas}values for the $^4F_{9/2}$ level indicates that the emission from this level is not fully radiative, suggesting the presence of some non-radiative decay contributions. Typically, non-radiative contributions may occur due to energy transfer among the Dy^{3+}ions or multiphonon relaxation, or a combination of both. In the current Dy^{3+}-doped LTT glass system, the decrease in measured lifetimes could be attributed to the role of energy transfer among the Dy^{3+}ions at higher concentrations.

4. Conclusions

The absorption and photoluminescence spectra of Dy^{3+}-doped LTT glasses at room temperature were recorded and analyzed using the Judd–Ofelt theory. The reasonably small δ_{rms} of ±0.34×10−6, obtained between the measured and calculated oscillator strengths, indicate the accuracy of J–O intensity parameters. The luminescence quenching of emission transitions originating from the $^4F_{9/2}$ excited state to its lower-lying states with an increase in Dy^{3+}concentration has been discussed. The Y/B luminescence intensity ratios suggest that Dy–O covalence increases with the rise in Dy^{3+}ion concentration. The color coordinates, evaluated for appropriate combinations of yellow-to-blue emissions, match with those in the white light region of the CIE chromaticity diagram. The higher values of branching ratios and stimulated emission cross-sections for the $^4F_{9/2}\rightarrow{}^6H_{13/2\ transition}$ indicate the potential utility of LTTDy10 glass as a laser material. For all $^{Dy3+}$concentrations, the fluorescence decay curves exhibit a single-exponential nature. The variation of lifetimes of the 4F9/2 excited level with Dy^{3+}concentration is attributed to the increasing interaction among Dy^{3+}ions at higher concentrations. This investigation suggests that LTT glasses doped with 1.25 mol% of Dy^{3+}ions could be useful as potential laser materials and for generating white light in color-displaying devices.

References

1. J.A. Savage, Mater. Sci. Rep. 2 (1987) 99.
2. J. Heo, M. Rodrigues, S.J. Saggese, G.H. Sigel Jr., Appl. Opt. 30 (1991) 3944.
3. Huang, L., Yamashita, T., Jose, R., Arai, Y., Suzuki, T., &Ohishi, Y. (2007). Intense ultraviolet emission from Tb3+ and Yb3+ codoped glass ceramic containing CaF2 nanocrystals. Applied physics letters, 90(13).
4. Basavapoornima, C., Jayasankar, C. K., &Chandrachoodan, P. P. (2009). Luminescence and laser transition studies of Dy3+: K–Mg–Al fluorophosphate glasses. Physica B: Condensed Matter, 404(2), 235-242.

5. Uma, V., Marimuthu, K., & Muralidharan, G. (2016). Influence of modifier cations on the spectroscopic properties of Dy3+doped telluroborate glasses for white light applications. Journal of fluorescence, 26(6), 2281-2294.
6. Khan, I., Rooh, G., Rajaramakrishna, R., Srisittipokakun, N., Kim, H. J., Kaewkhao, J., &Ruangtaweep, Y. (2019). Photoluminescence Properties of Dy 3+ Ion-Doped Li 2 O-PbO-Gd 2 O 3-SiO 2 Glasses for White Light Application. Brazilian Journal of Physics, 49, 605-614.
7. J. Heo, Y.B. Shin, J. Non-Cryst. Solids 196 (1996) 162.
8. P. Srivastava, S.B. Rai, D.K. Rai, Spectrochim. Acta A 59 (2003) 3303.
9. J. McDougall, D.B. Hollis, M.J.P. Payne, Phys. Chem. Glasses 35 (1994) 258.
10. K.K. Mahato, A. Rai, S.B. Rai, Spectrochim. Acta A 61 (2005) 431.
11. P. Nachimuthu, R. Jagannathan, V. Nirmal Kumar, D. Narayana Rao, J. NonCryst. Solids 217 (1997) 215.
12. Jayasimhadri M, Jang K, Lee HS, Chen B, Yi S-S, Jeong J-H (2009)White light generation from Dy3+-doped ZnO–B2O3–P2O5 glasses.J Appl Phys 106:13105–1310913.
13. Arunkumar S, Venkataiah G, Marimuthu K (2014) Spectroscopicand energy transfer behavior of Dy3+ions in B2O3–TeO2–PbO–PbF2–Bi2O3–CdO glasses for laser and WLED applications.Spectrochim Acta A 136:1684–169714.
14. Kumar MVV, Jamalaiah BC, Gopal KR, Reddy RR (2012) Opticalabsorption and fluorescence studies of Dy3+-doped leadtelluroborate glasses. J lumin 132:86–9015.
15. Shanmugavelu B, Ravi Kanth Kumar VV (2014) Luminescencestudies of Dy3+doped bismuth zinc borate glasses. J Lumin 146:358–36.
16. J. Qiu, K. Hirao, Solid State Commun. 106 (1998) 795.
17. J. Qiu, K. Miura, H. Inouye, Y. Kondo, T. Mitsuyu, K. Hirao, Appl. Phys. Lett. 73 (1998) 1763.
18. T. Katsumata, K. Sasajima, T. Nabae, S. Komuro, T. Morikawa, J. Am. Ceram. Soc. 81 (1998) 413.
19. N. Kodama, T. Takahashi, M. Yamaga, Y. Tanii, J. Qiu, K. Hirao, Appl. Phys. Lett. 75 (1999) 1715.
20. T. Kinoshita, M. Yamazaki, H. Kawazoe, H. Hosono, J. Appl. Phys.86 (1999) 3729.
21. D. Jia, R.S. Meltzer, W.M. Yen, Appl. Phys. Lett. 80 (2002) 1535.
22. T. Matsuzawa, Y. Aoki, N. Takeuchi, Y. Murayama, J. Electrochem.Soc. 143 (1996) 2670.
23. T. Aitasalo, P. Deren, J. Holsa, H. Jungner, J.C. Krupa,M. Lastusaari, J. Legendziewicz, J. Niittykoski, W. Strek, J. SolidState Chem. 171 (2003) 114.
24. Y. Murazaki, K. Arai, K. Ichinomiya, Jpn. Rare Earths 35 (1999) 41.
25. J.K. Park, C.H. Kim, S.H. Park, H.D. Park, S.Y. Choi, Appl. Phys.Lett. 84 (2004) 1647.
26. J.L. Sommerdijk, A. Bril, J. Electrochem. Soc. 122 (1975) 952.
27. K. Riwotzki, M. Haase, J. Phys. Chem. B 102 (1998) 10129.
28. F. Gu, S.F. Shu, M.K. Lu, G.J. Zhou, S.W. Liu, D. Xu, D.R. Yuan,Chem. Phys. Lett. 380 (2003) 185.
29. J. Kuang, Y. Liu, Chem. Lett. 34 (2005) 598.
30. M. Yu, J. Lin, Z. Wang, J. Fu, S. Wang, H.J. Zhnag, Y.C. Han,Chem. Mater. 14 (2002) 2224.
31. H. Choi, C.H. Kim, C.H. Pyun, S.J. Kim, J. Lumin. 82 (1999) 25.